A&A manuscript no.
(will be inserted by hand later)

Your thesaurus codes are:
03.13.4; 08(08.16.4; 08.05.3; 08.06.3)

ASTRONOMY
AND
ASTROPHYSICS
15.5.1998

New input data for synthetic AGB evolution

J. Wagenhuber and M.A.T. Groenewegen

Max-Planck-Institut für Astrophysik, Karl-Schwarzschild-Straße 1, D-85740 Garching, Germany

Received ; accepted

Abstract. Analytic formulae are presented to construct detailed secular lightcurves of both early asymptotic giant branch (AGB) and thermally pulsing AGB stars. They are based on an extensive grid of evolutionary calculations, performed with an updated stellar evolution code. Basic input parameters are the initial mass $M_{\rm i}$, $0.8 \leq M_{\rm i}/M_\odot \leq 7$, metallicity $Z_{\rm i} = 0.0001, 0.008, 0.02$, and the mixing length theory (MLT) parameter. The formulae allow for two important effects, namely that the first pulses do not reach the full amplitude, and hot bottom burning (HBB) in massive stars, which are both not accounted for by core mass - luminosity relations of the usual type.

Furthermore, the dependence of the effective temperature and a few other quantities characterizing the conditions at the base of the convective envelope, which are relevant for HBB, are investigated as functions of luminosity, total and core mass for different formulations of the convection theory applied, MLT or Canuto & Mazzitelli's (1991) theory.

Key words: Stars: AGB and post-AGB – Stars: evolution – Stars: fundamental parameters – Methods: numerical

1. Introduction

As a matter of fact, full AGB stellar evolution calculations are unable to provide the statistical information needed for purposes like population synthesis. There are three main reasons for this.

First, the calculations are rather lengthy, reflecting the complexity of the inner structure of AGB stars and of the temporal evolution due to thermal pulses (TPs, also called helium shell flashes; see e. g. Iben & Renzini 1983; Boothroyd & Sackmann 1988, in the following BS88; Lattanzio 1986, LA86; Wagenhuber & Weiss 1994,WW94; and Blöcker 1995, B95).

Second, the calculations involve at least two poorly known parameters, the mass loss efficiency η and the mass loss prescription, and the mixing length (MLT) parameter α, each of them only meaningful in the framework of the *a priori* chosen description of the mass loss and convection theory, respectively. Since it has become clear that AGB evolution is dominated by mass loss (Schönberner 1979), numerous formalisms giving the mass loss rate as a function of the stellar parameters have been applied (e.g. Reimers 1975, Iben & Renzini 1983, Mazzitelli & D'Antona 1986, Wood & Faulkner 1986, Vassiliadis & Wood 1993 VW93, B95). The uncertainties were cast into the "efficiency" parameter, which depends on the mass loss prescription used, and which is actually a parameter that can be calibrated from AGB population synthesis models (e.g. GdJ, Groenewegen & de Jong 1994).

In addition, the MLT parameter is related to a series of problems concerning (a) the correct effective temperature scale of late-type stars derived from observations, (b) the opacity at low temperatures (Alexander & Ferguson 1994), (c) the time-dependent problem of dust formation (Fleischer, Gauger & Sedlmayr 1992, and references therein), and (d) the theory of convection itself.

The third restriction of the use of full evolutionary calculations is the occurrence of the third dredge-up as a consequence of TPs, which is considered to be responsible for the formation of carbon stars. However, canonical stellar evolution calculations do not consistently predict the formation of carbon stars in the mass range that they are observed, roughly between 1.2-1.5 $M_\odot$ depending on metallicity and about 5 $M_\odot$ (e.g. GdJ, Groenewegen et al. 1995). The explanation is still under debate and recent progress has been made (see e. g. Frost & Lattanzio 1996, Staniero et al. 1997, Herwig et al. 1997) but not to the degree that the results can easily be included in synthetic AGB models. Therefore these models introduce a fudge parameter to describe the third dredge-up, in particular the dredge-up efficiency λ.

To summarize: In order to describe the evolution of whole stellar populations using synthetic calculations, one has to explore a parameter space with at least five dimensions: $(M_{\rm i}, Z_{\rm i}, \alpha, \eta, \lambda)$. This has been done in the past e. g. by Renzini & Voli (1981), Jørgensen (1991), Groenewegen & de Jong (1993, GdJ) and Marigo et al. (1996). Although these works have contributed a lot to an improved understanding of AGB evolution, there are some obvious shortcomings: e.g. the data collected by GdJ and frequently used since then are partially incomplete, making some *ad hoc* inter- and extrapolations necessary, since results obtained in three decades are combined

Send offprint requests to: M.A.T. Groenewegen. E-mail: groen@mpa-garching.mpg.de

with each other, and they are oversimplified in some respects, e. g. concerning hot bottom burning (HBB). Furthermore, some data such as the rapid luminosity variations during a TP were neglected by many authors, although they are needed for some of the applications mentioned below.

The aim of this paper is to provide essential theoretical data for applications like classical synthetic AGB evolution. In this sense this paper provides a fully updated and improved set of relations with respect to GdJ.

The paper is organized as follows. In the next section some terminology is introduced, and the intrinsic errors due to physical assumptions are discussed. After this, the full evolution calculations up to and along the early (E-)AGB are shortly described (Sect. 3). The fourth section contains the recipes necessary to construct the secular lightcurves on the TP-AGB as a function of time for all relevant initial total masses and metallicities. Finally, properties of the effective temperature and the conditions at the bottom of the convective envelope for various model assumptions are discussed in Sect. 5.

2. General remarks and computational details

2.1. Some definitions

Let us first define some quantities and index labels that are used throughout the rest of this paper.

A *thermal pulse cycle* (TPC) is the time interval from a local maximum of helium burning, through quiescent hydrogen burning, up to the next TP. All quantities that refer to a TPC as a whole are defined to be functions of the conditions at the beginning of the TPC. The *first TP* is the one in which the maximum (integrated) luminosity produced by He-burning exceeds the maximum H-burning luminosity prior to this for the first time. Previously there may be *"pre-pulses"*.

Uppercase letters denote quantities that depend *linearly* on parameters. Time intervals (in years) are denoted by τ, in particular the duration of a TPC, the *interpulse time*, by $\tau_{\rm ip}$. Luminosity and mass (L, M) are given in solar units as usual, temperatures T in K, the abundances of hydrogen X, helium Y and metals Z in relative mass units ($X + Y + Z = 1$), and all others in cgs units.

Lowercase letters are used for decadic logarithms of the above quantities, e. g. $l \equiv \lg L/L_\odot$, except for $z \equiv \lg Z/0.02$ being the logarithmic metallicity scaled to solar.

The *core* is defined to be the part of a star inside the location where the local hydrogen content reaches half the photospheric value. Since the H-burning shell is extremely narrow (both in radius and relative mass units), this essentially coincides with all other definitions of the core mass in the literature. The *core growth* $\Delta M_{\rm c}$ is defined as $\int \max\{\frac{{\rm d}M_{\rm c}}{{\rm d}\tau}, 0\}{\rm d}\tau$. Usually, $\Delta M_{\rm c} = M_{\rm c}(\tau) - M_{\rm c,0}$, where $M_{\rm c,0}$ is the core mass at the first TP.

The *mantle* is the part between the photosphere and the core. In terms of the relative mass content, it is almost identical with what is frequently called "(convective) envelope".

One has to distinguish three different TP-AGB phases, defined in WW94. There are:

(i) The *transition phase* from the E-AGB to the first TP, in which pre-pulses may take place.
(ii) The *turn-on phase*, comprising about the first ten TPs. All global quantities are aiming at their asymptotic behaviour, but still the deviations are significant (up to 60%). This is called *turn-on effect* or TOE here.
(iii) The *asymptotic phase*, where the global quantities have reached their asymptotic behaviour.

The MLT parameter α may be defined either for the MLT or Canuto & Mazzitelli's (1991) theory (CMT) and is labelled accordingly, if necessary.

The three sets of calculations for $Z_{\rm i} = 0.02, 0.008$ and 10^{-4} are called *pop I, LMC* and *pop II* in the following, respectively.

Subscripts:

b: Quantities defined at the bottom of the convective mantle,
c: concerning the core and
m: the mantle.

A,**B**,**C**,**D**: Denote luminosity extrema in the TPC (Fig. 1):
A - the *"slow maximum"* during quiescent H-burning,
B - the *"rapid dip"* following a TP,
C - the *"rapid peak"* after this,
D - the *"slow dip"* at the transition from He- to H-burning.

i: Initial values on the ZAMS, and
f: final values after the TP-AGB phase.
H: Something produced by or related to hydrogen or
He: helium burning.
0: Quantities at the beginning of an evolutionary phase as a whole, like the E-AGB and the TP-AGB,
TP: at the beginning of a TPC, and
1: at the end of the corresponding phase.
*: Denotes "effective" values measured at the photosphere.

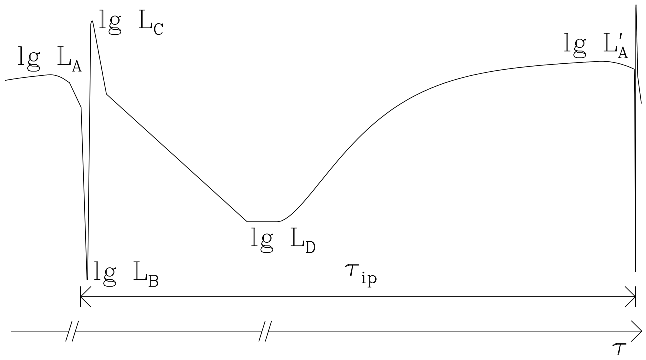

Fig. 1. A typical TPC as produced by the code described in the text. The labels illustrate some of the definitions in sect. 2.1. The time axis has been stretched around the first TP shown.

2.2. Intrinsic errors and physical assumptions

About 40 model sequences were run, with varying initial mass, metallicity or physical input parameters. Initial masses are between $0.8 \leq M_\mathrm{i} \leq 7$, the metallicity is $Z_\mathrm{i} = 0.02, 0.008, 0.0001$. The standard values for Y on the main sequence were 0.28, 0.2651 and 0.25 for pop I, LMC and pop II, respectively. The metal mix is according to Anders & Grevesse (1989) for pop I, scaled by the appropriate factor for pop II, and according to Russell & Bessell (1989) combined with Russell & Dopita (1990) for the LMC models.

During the full stellar evolution model calculations new input physics became available which allowed us to test for any differences indiced by them. Two different physical models were used for the pop I calculations and $M_\mathrm{i} \in \{1, 1.5, 2, 3, 5, 7\}$: one with nuclear equilibrium rates and opacities from the collection of older opacity tables by Weiss, Keady & Magee (1990), as explained in WW94, and the other one with a nuclear network, and more recent opacities taken from Rogers & Iglesias (1992), in the following referred to as models A and B, respectively. For $T < 10^4$K, the OPAL tables were completed by LAOL data. Both sets agree well around $T \approx 10^4$K. The LMC calculations were carried out with model A, model B was employed for pop II. The network comprises the following species relevant for the AGB: ^{1}H, ^{3}He, ^{4}He, ^{13}C, ^{14}N, ^{15}N, ^{17}O, and $^{12}\mathrm{C} + n\,\alpha, n \leq 3$. A leakage out of the CNO cycle, which is unimportant for the energy generation rate (Mowlavi, Jorissen & Arnould 1996), was not taken into account. For more details, see Weiss & Truran (1990), Weiss, Wagenhuber & Denissenkov (1996) and Wagenhuber (1996). The models were evolved off the ZAMS through the core helium flash (for $M_\mathrm{i} \leq 2$) up to the AGB without manual interventions and with a high numerical resolution (see WW94).

When comparing model A and B calculations, one finds as the major effect that for $M_\mathrm{i} \gtrsim 4$ the initial core mass $M_\mathrm{c,0}$ as a function of M_i increases slightly faster for model B than for model A (see Fig. 7). The greatest difference of $0.08 M_\odot$ occurs for $M_\mathrm{i} = 7$ (the OPAL data for $M_\mathrm{c,0}$ agree with those of DAM96 to within $0.01 M_\odot$). Accordingly, the massive stars in model B reach somewhat higher luminosities than their siblings in model A with the same M_i. Some of the model B sequences experience "breathing pulses" (Castellani et al. 1985) at the end of convective core helium burning, which slightly increase $M_\mathrm{c,0}(M_\mathrm{i})$. Since there is a tendency that they do not take place in our code if the spatial and temporal resolution is increased early enough in the evolution, they may be of pure numerical origin. However, on the TP-AGB luminosities and time scales, *when considered as functions of* M_c *and* ΔM_c, agree with each other to within 12%, the main contribution being that the TOE tends to be stronger for model B. One exception is discussed in section 4.4.

The standard choice for the MLT parameter was $\alpha = 1.5$, which together with the adopted opacities for low temperatures yielded somewhat lower T_* when compared to results by D'Antona & Mazzitelli (1996, DAM96) and B95. The code used in the present work needs a MLT parameter approximately 0.25 and 0.2 larger, respectively, to reproduce their results. In order to fit the present sun with OPAL, $\alpha = 1.578$ and $Y = 0.2803$ is needed, very close to the standard values of 1.50 and 0.28, giving rise to a possible shift of T_* by far within the uncertainties of the observed AGB effective temperature scale. Since the dependence of all results on Z is the dominating one, uncertainties due to the variations of Y for a given Z of about ± 0.03 are neglected.

Additionally, some TPCs were repeated with the CMT formulation of convection instead of standard MLT. This was done with a mixing length Λ proportional to the local pressure scale heigth H_p, i. e. $\Lambda = \alpha_\mathrm{CMT} H_\mathrm{p}$. The choice $\alpha_\mathrm{CMT} = 0.65$ reproduced the effective temperatures obtained with MLT and $\alpha_\mathrm{MLT} = 1.5$ very well (see section 5.2). Beyond this, time-dependence according to the model by Arnett (1969) and a turbulent pressure model according to CMT were invoked in some test sequences. These tests reveal that the various convection formalisms, too, do not influence L and τ, by more than 2%, except if HBB is operating (see section 4.1). The time dependent convection models give rise to two interesting effects during the "rapid luminosity peak": T_* is cooler by about 100K than during the quiescent phases, and T_b of low-mass stars, which usually never exceeds 1.5×10^6K, reaches peak values of 5×10^6K shortly after a TP, since the bottom of the mantle convection zone cannot retreat as quickly as in the case of "instantaneous" convection. However, L_* and the TP timescales are unaffected.

These calculations furthermore allow to estimate the impact of the way the initial models were generated on the TP-AGB. Instead of full calculations through the core helium flash, often the chemical profile of the last model at the tip of the RGB (red giant branch), or an artificial step profile, are used to obtain a core helium burning model by means of an explicit integration method. These three possibilities have been carried out for a pop II, $M_\mathrm{i} = 1.25 M_\odot$ model. The luminosities at the onset of the core helium burning phases, which last for 62, 56 and 78 Myr, are 79.8, 81.1 and $82.3 L_\odot$ for the full evolution, H-profile and step profile cases, respectively. Only the latter experiences a breathing pulse. The beginning of the TP-AGB is shown in Fig. 2. The sequences evolved off artificial initial models show an irregular behaviour during the first TPCs. This leads to the conclusion that the composition profile of the H-shell provides a rather long-lasting memory, which may change L_* and τ_ip at the first TP by about 10%, and will therefore mildly influence the evolution of low-mass stars, since these experience only few TPs (GdJ).

2.3. Outline of the method

Here we briefly outline the method used to derive analytical relations from the full calculations, using the core mass-luminosity relation as an example.

It has been known for a long time that two important quantities characterizing the TP-AGB, L_A and $\lg \tau_\mathrm{ip}$, approximately are linear functions of the core mass (Paczyński 1970, 1975). However, many different formulae were published (e.g. Iben

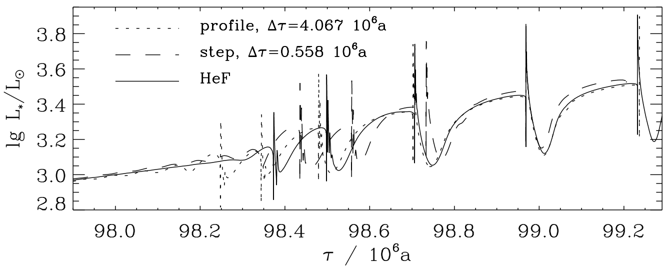

Fig. 2. The lightcurves during the first TPCs for the full evolution through the core helium flash (full line) and two cases of artificial initial models (see text). The time axis (in Myr since the onset of core helium burning) of the latter two has been shifted by the amount indicated so that the last but one TPs lie on top of each other.

& Truran 1978 (IT78), Wood & Zarro 1981 (WZ81), LA86, BS88).

To find an appropriate description of our data, first L and $\lg\tau$ were assumed to depend linearly on M_c, and each of the three sets of calculations (pop I, II and LMC) was considered separately (sometimes a quadratic dependance was found to be more appropriate). A random subset of data from TPCs in the asymptotic regime without HBB, distributed within $0.55 < M_c < 0.80$, was used to obtain a rough estimate for the coefficients, and to determine if the latter are constant, or depend linearly on Z_i or $\lg Z_i$. One thus obtains a first guess relation $g^{(1)}(M_c, Z_i)$.

Next, the residua due to the TOE are considered, still ignoring HBB for the moment. They can well be described by an exponentially decaying function of the core growth, i. e. the ansatz $g^{(2)} \approx \lg|f - g^{(1)}|$ is a linear function of ΔM_c, with coefficients depending on M_c or $M_{c,0}$ and Z_i or $\lg Z_i$, which are determined by a non-linear fit for a subset of all the data. To continue, the least significant terms in the new residual function are removed. The resulting formula is checked against the full available data set. One finds that the data points previously not taken into account are well predicted, with deviations of the order of less than twice the mean error with respect to the subset data.

The effects of HBB are strongly non-linear functions of the total mass and the MLT parameter α. One calculation with $\alpha = 2$ ($M_i = 5M_\odot$) was carried out, and data from DAM96 and B95 were additionally considered. A large number of analytic forms with the correct qualitative behaviour were tested.

In a final step, all coefficients are improved simultaneously by applying a non-linear fitting procedure to the complete data set. The values of the parameters are given with as many digits as necessary to obtain deviations of less than 1% with respect to results calculated with 16 digits. The number of digits must not be mistaken as an indication that the parameters are “known” to this precision, since changing one parameter usually could be compensated by changes of another one, at the expense that some data points were reproduced considerably worse.

2.4. Limits of applicability

All the formulae presented below should be considered as interpolations, valid for the parameter space $0.8 \lesssim M_i \lesssim 7$ and $10^{-4} \leq Z_i \lesssim 0.02$. Below $Z_i = 10^{-4}$, new physical effects occur (see Cassisi, Castellani & Tornambè, 1996) that partially invalidate the descriptions given below.

With the standard choice of the MLT-parameter, $\alpha = 1.5$, almost no HBB takes place, and the resulting T_* are close to the lower limit of the what is allowed by observations. Hence $\alpha < 1.4$ is meaningless. On the other hand, no data with $\alpha > 2.8$ are available, so that larger values should be avoided too.

3. The evolution prior to the first thermal pulse

In synthetic AGB evolution calculations, the evolution prior to the first TP must be taken into account to determine the total mass left at the onset of TPs.

3.1. Up to the core helium flash

Low-mass stars that experience the core helium flash may lose a significant amount of mass on the first giant branch. Jimenez & MacDonald (1997) give a core mass-luminosity relation (CMLR) for the RGB, which in terms of the variables introduced in section 2.1 ($m_c = \lg M_c$ etc.) reads:

$$l_* = 4.826 + 0.066 z_i - 0.01 z_i^2 + (3.186 - 0.129 z_i - 3.48 m_c) m_c, \quad (1)$$

and which reproduces the data of this work for $M_c \gtrsim 0.26$ so perfectly that there is no need to establish a new relation. Together with Eq. (6) below, Eq. (1) can be directly integrated to obtain $L_*(\tau)$. For the purposes of synthetic AGB evolution, the core mass at the instant of time when the helium flash occurs can be approximated by

$$M_{c,\mathrm{RGBtip}} = (0.454 - 0.023 z_i + 0.059 M_i) \times \left(1 - (0.033 - 0.008 z_i) e^{M_i}\right), \quad (2)$$

which has a maximum of $M_{c,\mathrm{RGBtip}}$ approximately at an initial mass of

$$M_{i,\max} = -\ln(0.0169 - 0.005 z_i) - 2.935 - 0.022 z_i. \quad (3)$$

For $M_i < M_{i,\max}$, $M_{c,\mathrm{RGBtip}} = M_{c,\mathrm{RGBtip}}(M_{i,\max})$ must be used.

When $M_{c,\mathrm{RGBtip}} \lesssim 0.35$ according to Eq. (2), helium ignites under non-degenerate conditions, and there is no real RGB. This is the case for $M_i \gtrsim 2.5$. For $M_i \leq 1.5$, there is no systematic difference between OPAL and LAOL calculations ($\Delta M_c \leq 0.005$). The transition from degenerate to non-degenerate ignition turns out to be relatively model dependent. However, this does not affect the AGB, since for $M_i \gtrsim 2$ the RGB tip luminosity does not exceed $1500 L_\odot$, and the transition timescales from degenerate to non-degenerate are relatively short, so that almost no mass is lost.

The following core helium burning phase does not directly influence the AGB, since the luminosities are too low to drive significant mass loss, except for blue horizontal branch stars with an already very small mantle mass. These may directly evolve upward in the HRD and form AGB manquée stars, which are not further considered here.

3.2. The E-AGB

After core helium exhaustion, the helium shell initially burns quiescently. The first TP occurs when the He-exhausted core approaches the H-shell, at $M_{\rm H} - M_{\rm He} \lesssim 10^{-2}$. L_* rises from the relatively low values typical for convective core helium burning up to the high AGB luminosities. Since the evolutionary time scales on the E-AGB are long compared to TP recurrence times, and since for stars with $M_{\rm i} \gtrsim 4$ the maximum luminosity attained on the E-AGB exceeds the luminosity at the first TP, a considerable amount of mass may be lost already on the E-AGB. This is interesting with respect to the initial-final mass relation, since for $M_{\rm i} \approx 4$ there are indications that the final mass is less or comparable to the core mass at the first full thermal pulse (VW93).

On the E-AGB, there are competing contributions from H- and He-burning, depending on $M_{\rm i}$ and the evolutionary phase, so that it makes no sense to use a CMLR. Instead, the normalized E-AGB luminosity $l_{\rm E}$ is described directly as a function of the E-AGB phase $\phi_{\rm E} \equiv (\tau - \tau_0)/(\tau_1 - \tau_0)$, $0 \le \phi_{\rm E} \le 1$:

$$l_{\rm E} \;\equiv\; \frac{l_* - l_0}{l_1 - l_0} \;=\; v\phi_{\rm E} \,+\, (1-v)\phi_{\rm E}^{\beta}. \qquad (4)$$

The logarithmic luminosities at the beginning and the end of the E-AGB, respectively, and the mass of the helium exhausted core at the beginning of the E-AGB, $M_{\rm He,0}$, can be approximated by piecewise linear functions of the form $a_i + b_i z_{\rm i} + (c_i + d_i z_{\rm i}) M_{\rm i}$. The same holds for the depth of the luminosity dip that for massive stars occurs between the luminosity maximum on the E-AGB at τ_1 and the first TP. Once $M_{\rm He,0}(M_{\rm i}, Z_{\rm i})$ is given, the duration of the E-AGB, $\tau_1 - \tau_0$, and the two parameters v and β in Eq. (4) are approximately piecewise linear functions of $M_{\rm He,0}$ alone, independent of $Z_{\rm i}$. We find that $\lg(\tau_1 - \tau_0) = \max\left((8.4 - 5.0 \times M_{\rm He,0}), (7.6 - 3.1 \times M_{\rm He,0})\right)$, $v = \max\left(0.19, (-0.23 + 1.35 \times M_{\rm He,0})\right)$ and $\beta = \max\left((16.3 - 34.1 \times M_{\rm He,0}), 5.7\right)$ for $M_{\rm He,0}$ varying between 0.14 and 0.56.

4. The luminosity on the TP-AGB as a function of time

4.1. The core mass - luminosity relation (CMLR)

One of the most important relations that come out of evolutionary calculations is the maximum luminosity during quiescent H-burning, here referred to as $L_{\rm A}$, for which the following expression according to Sect. 2.3 is derived:

$$
\begin{aligned}
L_{\rm A} = \;& (18\,160 + 3980 z_{\rm i})(M_{\rm c} - 0.4468) && \text{(5a)}\\
& + \; 10^{2.705 + 1.649 M_{\rm c}} \times && \text{(5b)}\\
& \quad \times \left(10^{0.0237(\alpha - 1.447) M_{\rm c,0}^2 M_{\rm m}^2 (1 - {\rm e}^{-\Delta M_{\rm c}/0.01})}\right) && \text{(5c)}\\
& - \; 10^{3.529 - (M_{\rm c,0} - 0.4468)\Delta M_{\rm c}/0.01}. && \text{(5d)}
\end{aligned}
$$

The first term is recognized as the usual linear CMLR, but the slope is flatter than usual. The term (5b) provides a correction: For $M_{\rm c} \gtrsim 0.6$, when added to (5a), with (5c) set to unity, it yields the same numerical values for $L_{\rm A}$ as most CMLRs that were fitted for low core masses. On the other hand, for $M_{\rm c} \gtrsim 0.95$, the sum of the two terms (dotted lines in Fig. 3) approaches the formula given by IT, which is applicable for massive cores only.

The term (5c) corrects for HBB, which is characterized by a steep initial increase of $L_{\rm A}$, and a drop when the mantle mass $M_{\rm m}$ is reduced (B95, their figure 9). The calculations by DAM96 for $M_{\rm i} < 5$ show that HBB operates only for massive cores and mantles. The factor $(1 - {\rm e}^{-\Delta M_{\rm c}/0.01})$ mimics the initial increase of L_*, which levels out after about the first ten TPs. HBB strongly depends on the MLT parameter, with the results of DAM96 that made use of the CMT being described by $\alpha_{\rm MLT} = 2.75$. The data given by VW93 (their figure 12), not used in Eq. (5), are remarkably well reproduced by the choice $\alpha = 2.25$.

The last term, (5d), corrects for the TOE, which is quite important for $M_{\rm c} \lesssim 0.65$, and independent of Z. Figure 3 clearly shows that the CMLRs by WZ81 and LA86 are influenced by the TOE for low core masses.

4.2. The core growth equation

The equation that describes the core growth reads:

$$\frac{{\rm d}M_{\rm c}}{{\rm d}t} = \frac{q}{X_{\rm m}} L_{\rm H}, \qquad (6)$$

where q, the mass burnt per unit energy release, turns out to be slightly metallicity dependent due to the contribution from the pp-cycle for low Z. The calculations with a nuclear network yield the mean value $q = ((1.02 \pm 0.04) + 0.017z)10^{-11}$ ($M_\odot / L_\odot$yr). The luminosity produced by H-burning that enters Eq. (6) is smaller than the total luminosity, since gravitational energy release due to the core shrinking and the flow of burnt mantle material down to the core, together with relic helium burning, additionally contribute during quiescent H-burning:

$$\lg(L_{\rm H,A}/L_{\rm A}) = -0.012 - 10^{-1.25 - 113\Delta M_{\rm c}} - 0.0016 M_{\rm m}. \qquad (7)$$

This equation was derived for the standard value of the MLT parameter, which implies that the value of $L_{\rm A}$ to be used in Eq. (7) should be calculated from Eq. (5), with the term (5c) put to unity as the standard models did *not* experience any HBB.

4.3. Further relations for luminosity extrema

The first observable effect of a TP is that the layers above the helium shell source expand, thus the hydrogen shell is extinguished and the total luminosity drops. This *"rapid dip"* is the more pronounced the smaller the mantle mass is, since the inner layers of the mantle act as a reservoir of thermal energy that partly compensates the initial fast luminosity drop. The rapid dip is utterly unimportant for the secular evolution due to its very short duration, but during this phase $|{\rm d}L_*/{\rm d}t|$ reaches the

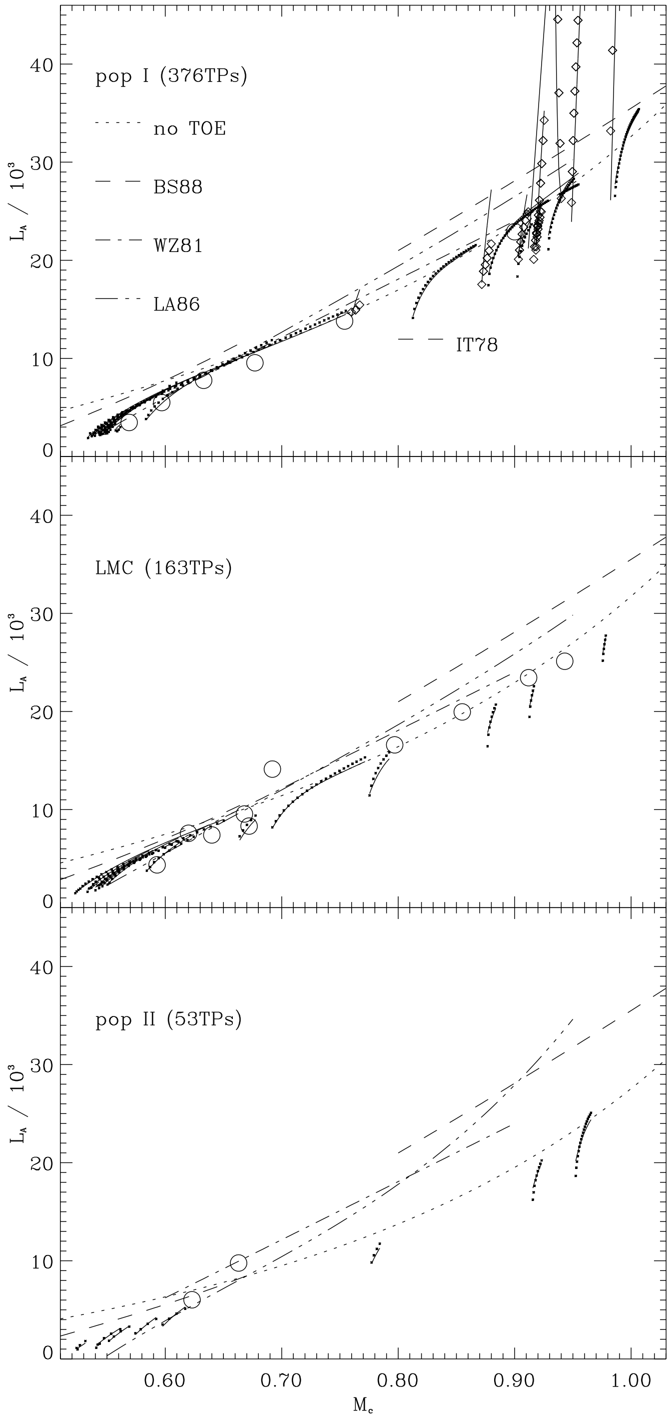

Fig. 3. The maximum luminosity during quiescent hydrogen burning as a function of the core mass and metallicity. *Dots*: data points extracted from the calculations with $\alpha_{\rm MLT} = 1.5$; $\diamond$: data for $\alpha_{\rm MLT} > 1.5$ from the calculation with $M_{\rm i} = 5$, DAM96 and B95. *Full lines* show the fit to the data given by Eq. (5). $\bigcirc$: independent data, *not* used for the fit, from Vassiliadis & Wood (1994) for post-AGB nuclei, i. e. objects with a vanishing mantle mass. The fit for this case, and without TOE, is shown by the *dotted lines*. The *other lines* represent CMLRs by various authors. For the formulae by Boothroyd & Sackmann (1988, BS88) and Lattanzio (1986, LA86) the dependence on μ, $Z_{\rm CNO}$ and Y, respectively, has been taken into account approximately.

highest values a single low-mass star can achieve. A fraction of roughly 10^{-3} of all pulsating AGB stars are expected to show corresponding rapid period changes. The fit formula given below strongly depends on $M_{\rm m}$ even for low core masses:

$$L_{\rm B} = \left(4.81(M_{\rm c} - 0.4865) + M_{\rm m}^{0.393}\right) \times \quad (8a)$$
$$\left(10^{2.879 + M_{\rm c}} - 10^{3.287 - (M_{\rm c,0} - 0.4865)\Delta M_{\rm c}/0.01}\right). \quad (8b)$$

After the rapid dip, for $M_{\rm c} \lesssim 0.7$ the layers above the inactive H-shell start to contract, therefore releasing gravitational energy; for heavier cores, L_* simply follows $L_{\rm He}$ after a short thermal adjustation phase. In either case a *"rapid peak"* emerges, in which the maximum total luminosity exceeds the quiescent H-burning luminosity prior to the TP, except for the very first weak TPs or in the case of strong HBB. Note that in many earlier calculations these peaks were suppressed for large mantle masses due to an insufficient numerical resolution. It turns out that a HBB term does not improve the fit, and is therefore left out:

$$L_{\rm C} = 59\,200\,M_c^2 - 10\,950 - \quad (9a)$$
$$10^{2.559 + 1.951 M_{\rm c,0} + (44.7 + (2254 Z_{\rm i} - 147.6) M_{\rm c,0})\Delta M_{\rm c}} \quad (9b)$$

Here Eq. (9b) accounts for the TOE, which vanishes for $\Delta M_{\rm c} \gtrsim 0.03$. In the asymptotic regime, the data nicely follow a quadratic relation (Fig. 4). $L_{\rm C}$ is an interesting quantity for two reasons. First, the rapid peak is the only mechanism capable of populating a high luminosity tail in the luminosity function of a sufficiently large sample with $M_{\rm i} \lesssim 3$. Second, if it should be true that an avalanche mass loss starts as soon as some luminosity threshold is exceeded (Tuchman, Sack & Barkat 1979), this would take place for the first time during a rapid peak, unless HBB is operating so effectively that $L_{\rm A} > L_{\rm C}$. It is a question of the interplay between the mass loss time scale and the duration of the peak, if such a gasping mass loss episode influences the secular evolution.

Finally, the helium burning declines and the H-shell recovers, giving rise to an extended and long-lasting *"slow dip"*. During the quiescent part of a TPC, $L_{\rm D} < L_* < L_{\rm A}$. The fit, like Eqs. (8) and (9), needs no HBB correction:

$$L_{\rm D} = (76360 + 6460 z_{\rm i})(M_{\rm c} - 0.3881)^2 - \quad (10a)$$
$$10^{1.55 + 2.11 M_{\rm c,0} + (59.7 - 119.8 M_{\rm c,0})\Delta M_{\rm c}}. \quad (10b)$$

4.4. The core mass-interpulse time relation

The second most important quantity to come out of evolutionary calculations is the core mass-interpulse time relation. The following relation is found:

$$\lg \tau_{\rm ip} = (-3.628 + 0.1337 z_{\rm i})(M_{\rm c} - 1.9454) - \quad (11a)$$
$$10^{-2.080 - 0.353 z_{\rm i} + 0.200(M_{\rm m} + \alpha - 1.5)} - \quad (11b)$$
$$10^{-0.626 - 70.30(M_{\rm c,0} - z_{\rm i})\Delta M_{\rm c}}. \quad (11c)$$

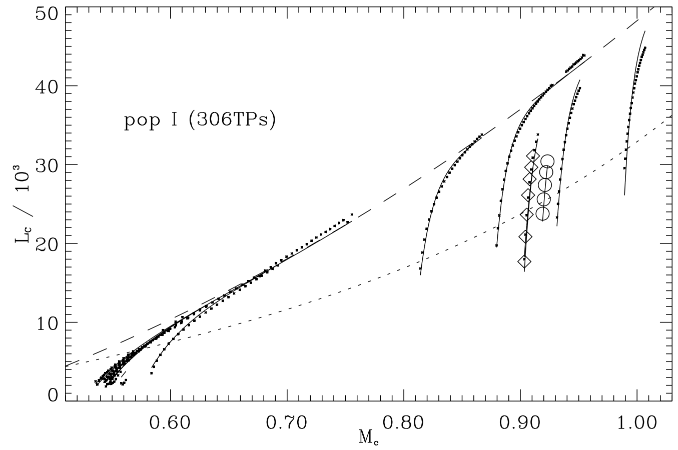

Fig. 4. The luminosity peak after a TP as a function of the core mass for $Z_i = 0.02$. *Dots*: data points from the calculations with $\alpha_{MLT} = 1.5$; $\diamond$: $\alpha_{MLT} = 2$, $\bigcirc$: data from DAM96, both not used for the fit, which is shown by *full lines*. The *dotted line* depicts L_A without TOE and HBB as in Fig. 3. The *dashed line* is the asymptotic relation Eq. (9a).

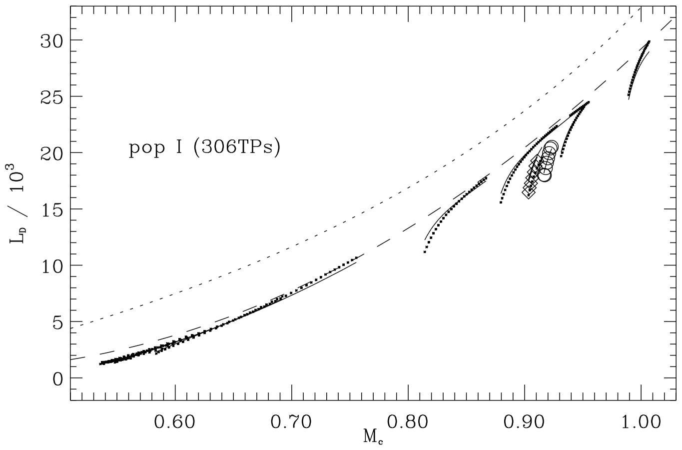

Fig. 5. The minimum luminosity at the beginning of a TPC as a function of M_c for Z_i = 0.02. *Dashed line*: Eq. (10a), other symbols: see Fig. 4.

Again, Eqs. (11b) and (11c) account for HBB and the TOE, resp. Interestingly, Eq. (11) predicts the recurrence time of prepulses with $M_c < M_{c,0}$ (crosses in Fig. 6). For $M_c \lesssim 0.7$ and in the asymptotic regime, the results of the present work agree well with relations for τ_{ip} given by BS88 and WZ81. However, the latter disagree for $M_c > 0.8$, and give lower and upper limits only, respectively.

Compared to the asymptotic exponential relation, the TOE reduces τ_{ip} by almost a factor of two. The influence of Z_i on τ_{ip} is rather strong, in the sense that the interpulse times increase with decreasing metallicity. This also means that the He-shell accretes material processed by the H-shell for a longer time, so that the TPs become more violent. The reason is that the plasma in a typical pop II He-shell is more degenerate than in a pop I-shell. An important consequence is that the third dredge-

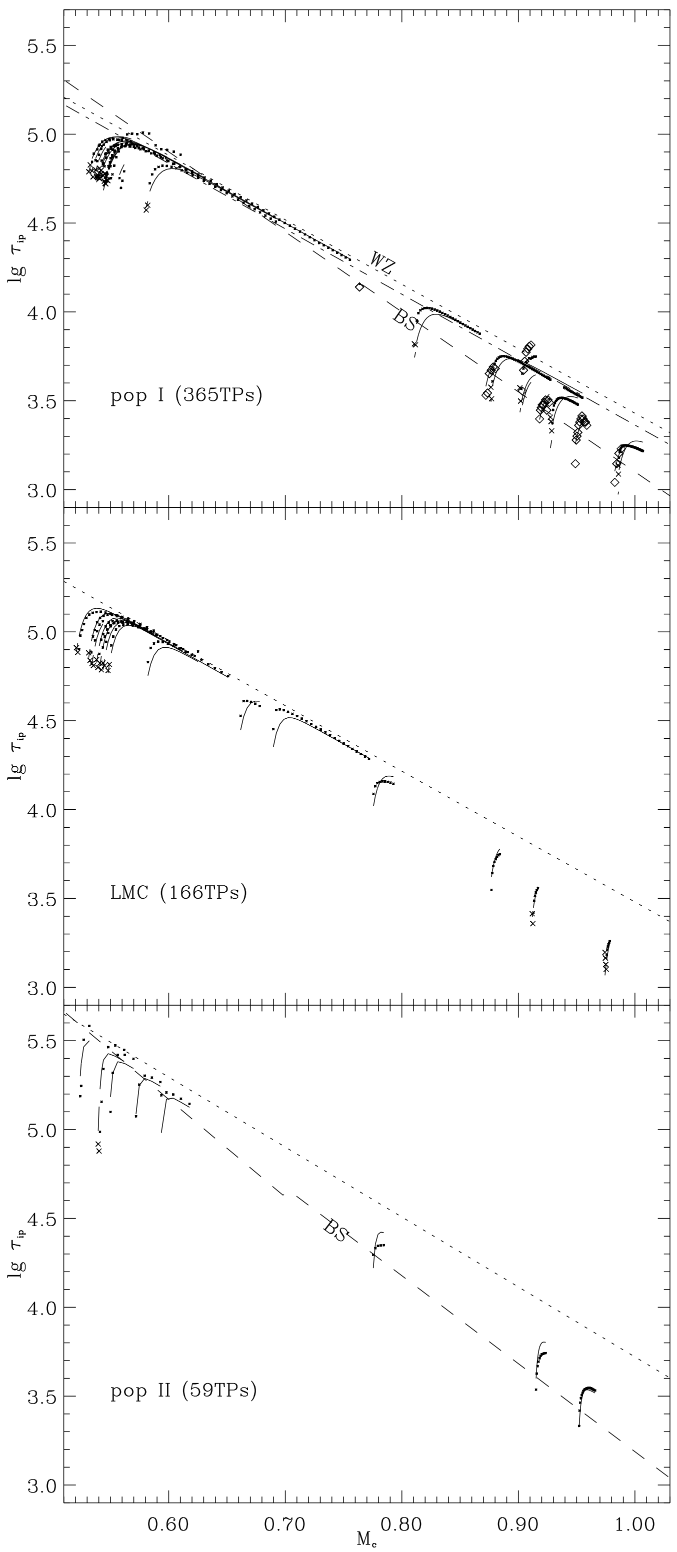

Fig. 6. The interpulse time as a function of the core mass and metallicity. Data points taken from the calculations, used for the fit, are shown as *dots*, the values given by Eq. (11) as *full lines*. $\diamond$: data from DAM96, and from the run with α_{MLT} = 2, M_i = 5 ($M_c \gtrsim 0.9$). $\times$: recurrence time of pre-pulses, not used for the fit. *Dashed* and *dash-dotted* lines: relations from BS88 and WZ81, respectively. *Dotted* lines: the asymptotic relation Eq. (11a).

up occurs the earlier, i.e. for lower core masses, the lower the metallicity.

A further quantity needed to construct secular lightcurves is the time τ_D that elapses between a TP and the slow dip, i.e. when $L_* = L_D$. We find

$$\lg(\tau_D/\tau_{ip}) = -1.01 + 0.20\, z_i\,(M_c - 1). \quad (12)$$

4.5. The core mass at the first thermal pulse

There is one quantity of outstanding importance left to be discussed, the core mass at the first TP, i. e. $M_{c,0}(M_i, Z_i)$. It determines the minimum remnant mass, and is therefore closely connected to the initial-final mass relation. For $M_i \lesssim 2$, the stars develop very similar degenerate He-cores (see section 3.1), and all end up with $M_{c,0} \approx 0.55$. On the other hand, massive stars with $M_i \gtrsim 4.5$ experience the second dredge-up, which shifts the H-He-discontinuity inward (in mass), with the resulting $M_{c,0}$ being a linear function of M_i. In between, there is a transition region, which is rather strongly influenced by computational details. For stars in this transition region, $\mathrm{dM_{c,0}/dM_i} \gtrsim 0.25$, and since L_* increases strongly with M_c, and the mass loss even much more steeply with L_*, such transition stars, despite their larger mass reservoir, have a *shorter* AGB lifetime than slightly less massive counterparts. In WW94 the following parametrization was introduced:

$$M_{c,0}(M_i) = \left(-p_1(M_i - p_2)^2 + p_3\right) f + \quad (13a)$$

$$(p_4 M_i + p_5)(1 - f), \qquad \text{where} \quad (13b)$$

$$f(M_i) = \left(1 + \mathrm{e}^{\frac{M_i - p_6}{p_7}}\right)^{-1}. \quad (13c)$$

Equation (13a) mimics $M_{c,0}$ for stars with $M_i < 2.5$ that experience the core helium flash, which is almost constant. Eq. (13b) accounts for the linear ingress of the second dredge-up for $M_i \gtrsim 4.5$, and Eq. (13c) mediates. All parameters can be interpolated linearly in $\lg Z_i$, hence in Table 1 their numerical values are given for two standard metallicities only.

A compilation of data from various authors is shown in Fig. 7. There is a tendency that more recent opacities yield higher values of $M_{c,0}$. Blöcker's (B95) data points lie systematically below all other's. Obviously there is no systematic effect due to the inclusion of semiconvection (LA86, DAM96). The compilation by GdJ systematically deviates from the data for the LMC metallicity in the sense that for low-mass stars it predicts too large values of $M_{c,0}$.

Pop	p_1	p_2	p_3	p_4	p_5	p_6	p_7
I	0.0294	1.478	0.550	0.0634	0.572	3.193	0.260
II	0.0213	2.589	0.592	0.0324	0.790	2.867	0.260

Table 1. The coefficients of Eq. (13) for $Z_i = 0.02$ and 10^{-4}.

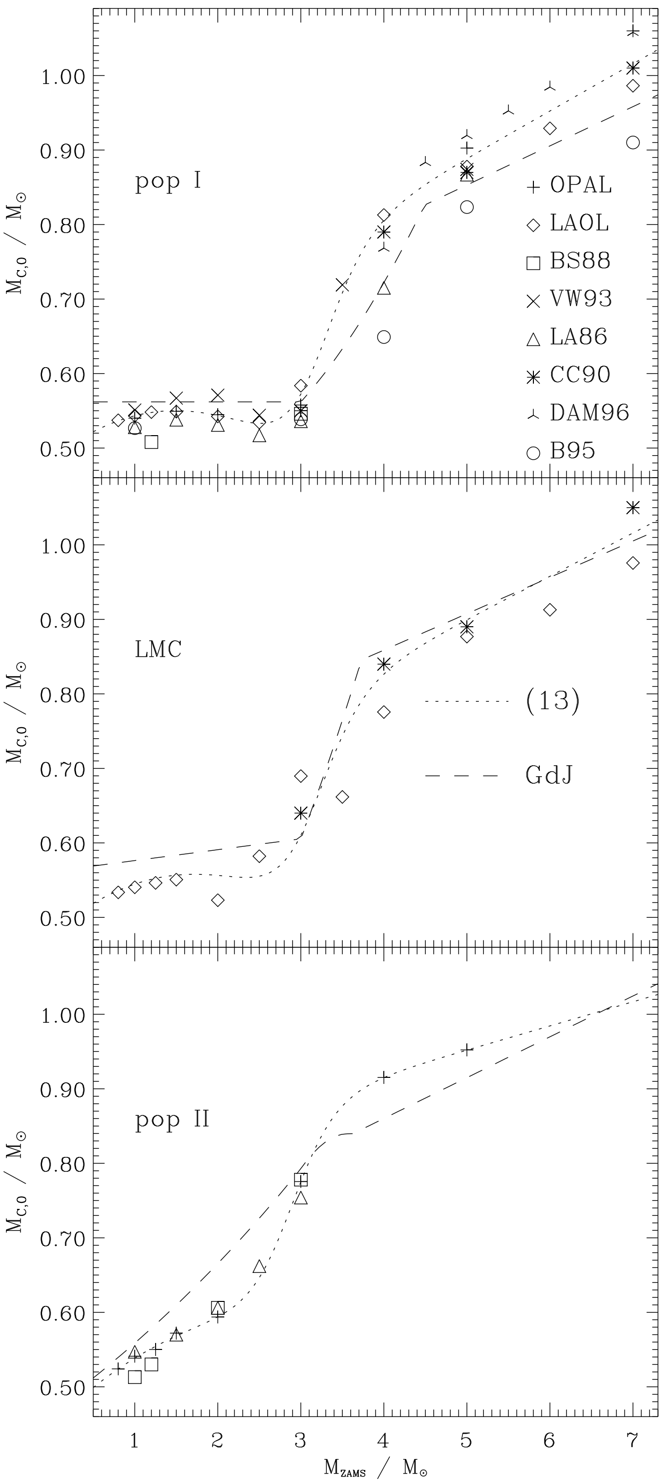

Fig. 7. The core mass at the first TP as a function of the initial mass and metallicity. The symbols show data from various authors (CC90: Castellani, Chieffi & Straniero, 1990). The lines show the relation (13a, dots) and the one used by GdJ (dashed).

4.6. Luminosity variations during the thermal pulse cycle

In previous synthetic AGB calculations, the luminosity variations during a thermal pulse cycle were either neglected (Renzini & Voli 1981), or described by simple stepfunctions (GdJ, Marigo et al. 1996). This is clearly insufficient if accurate theoretical luminosity functions are to be predicted. This section completes the description of $L_*(\tau)$ on the AGB.

At the instant of time when $L_* = L_\mathrm{D}$, i. e. in the slow dip, the H-shell is recovering from the preceding TP, and $L_\mathrm{H} \approx L_\mathrm{He}$. It turns out that the luminosity produced by H-burning that enters Eq. (6), when normalized to the value predicted by the CMLR Eq. (5) and Eq. (7), has an almost universal form (see also WZ81), independent of Z_i. Let $\phi \equiv \tau/\tau_\mathrm{ip}$ ($\phi = 0$ at the TP initiating the TPC, when $M_\mathrm{c} = M_\mathrm{c,TP}$). Then we define

$$h_\mathrm{H}(\phi) \equiv \frac{L_\mathrm{H}(\phi)}{L_\mathrm{H,CMLR}(M_\mathrm{c}(\phi), M_\mathrm{c,0}, M_*)} = \frac{1 - \mathrm{e}^{-\beta_\mathrm{H}\phi^2}}{1 - \mathrm{e}^{-\beta_\mathrm{H}}}, \qquad (14)$$

where $\beta_\mathrm{H} = 93.11(M_\mathrm{c,TP} - 0.4569)$. There are small systematic deviations for the first TP of each sequence, which, however, have no influence on the integration of Eq. (6).

L_* depends similarly on ϕ. In the following, the arguments of quantities given by a CMLR are omitted; the index "TP" denotes a quantity as given by the corresponding CMLR for $M_\mathrm{c} = M_\mathrm{c,TP}$. The form function h_L is given by

$$h_\mathrm{L}(\phi) \equiv \frac{L_*(\phi)\frac{L_\mathrm{A,TP}}{L_\mathrm{A}(M_\mathrm{c}(\phi))} - L_\mathrm{D,TP}}{L_\mathrm{A,TP} - L_\mathrm{D,TP}} = \frac{1 - \mathrm{e}^{-\beta_\mathrm{L}\phi_*^{b_\mathrm{L}}}}{1 - \mathrm{e}^{-\beta_\mathrm{L}}}, \qquad (15)$$

where $\beta_\mathrm{L} = 7.95$ and $b_\mathrm{L} = 2.13\,(1.331 - M_\mathrm{c,TP})$, and $\phi_* \equiv \max\{\phi - 0.1, 0\}$ accounts for the behaviour shortly after the slow dip. Note that $h_\mathrm{L}(1) > 0.999 \approx 1$, and that $0.1 \lesssim \phi < 1$ due to Eq. (12).

Let now $\tilde\phi \equiv (\tau - \tau_\mathrm{C})/\tau_\mathrm{ip}(M_\mathrm{c}, M_\mathrm{c,0}, M_*)$ be a shifted TPC phase, so that $\tilde\phi = 0$ at the rapid peak when $L_* = L_\mathrm{C}$. The peak itself can be approximated by a parabola, followed by an exponential decline. The luminosity from the rapid peak until $L_* = L_\mathrm{D}$ can well be described by:

$$l_*(\tilde\phi) = \lg L_\mathrm{C} - \begin{cases} a\tilde\phi^2, & \text{if } \tilde\phi \le \frac{b}{2a}, \\ b\tilde\phi - \frac{b^2}{4a}, & \text{if } \tilde\phi \le \frac{b}{4a} + \frac{\Delta_\mathrm{N}}{b}, \\ \Delta_\mathrm{N}(1 - f_\mathrm{N}) - f_\mathrm{N}\left(-b\tilde\phi + \frac{b^2}{4a}\right) & \text{else.} \end{cases} \qquad (16)$$

The physical meaning of Δ_N and f_N is, that when the luminosity $l_* = \lg L_\mathrm{C} - \Delta_\mathrm{N}$ is reached, the time scale for the decline changes from τ_ip/b to $\tau_\mathrm{ip}/(f_\mathrm{N} b)$. The parameters $\lg a, \lg b, \lg \Delta_\mathrm{N}$ and $\lg f_\mathrm{N}$ are functions of Z_i, M_c and $M_\mathrm{c,0}$ and can again be described by linear relations with a TOE correction for $\lg a$ and $\lg b$. They obey the simplified relations

$$\lg a = 7.23 - 4.40\,M_\mathrm{c}, \qquad (17)$$
$$\lg b = 3.30 - 2.91\,M_\mathrm{c}, \qquad (18)$$
$$\lg \Delta_\mathrm{N} = 0.08 - 1.50\,M_\mathrm{c}, \quad \text{and} \qquad (19)$$
$$\lg f_\mathrm{N} = -1.84 + 1.79\,M_\mathrm{c}. \qquad (20)$$

Note that the duration of the rapid peak does not scale like τ_ip. Relative to τ_ip, it lasts the longer the more massive the core is, i. e. the shorter τ_ip.

5. Properties of the mantle

5.1. The method

Several physical aspects of AGB evolution depend on properties that are almost exclusively determined by the mantle. The justification is, that as long as there is a radiative transition region between the core and the lower boundary of the mantle convection zone, the influence of the two outer boundary conditions on the core is negligible (WZ81). On the other hand, since the luminosity is essentially constant, the core, which prescribes L, can to first order be considered to be just a gravitating point source for the mantle.

Now consider L_*, M_*, M_c and the chemical composition to be given. The latter, owing to mixing during earlier evolutionary phases, is homogeneous up to and including the upper parts of the H-shell. Two outer boundary conditions for the mantle are given immediately: the effective stellar surface radius R_* is given by the Stefan-Boltzmann law and from some model for the optically thin outer envelope one can derive $P_*(L_*, M_*, T_*)$. By assuming a value for T_*, the four stellar structure equations for L, T, P (or ρ) and R as functions of the Lagrangean mass coordinate M_r can now be integrated inward. The transition to the core is well defined (see also Wagenhuber & Tuchman 1996) by a very steep rise of T and P by one and four, resp., orders of magnitude or more. In this way, a relation $M_\mathrm{c}(T_*)$ is defined that can be inverted numerically to yield T_* as a function of all other quantities, defining a three dimensional manifold in the four dimensional parameter space $(T_*, L_*, M_*, M_\mathrm{c})$. Full stellar evolution calculations of course establish a connection between L_* and M_c. In order to study pure mantle properties, however, it is much more convenient to treat them as independent variables to get rid of the complicated time dependent problem one is confronted with in full calculations.

In the following, a set of data relevant for HBB is discussed, together with *consistent* effective temperatures, for various model assumptions that made use of OPAL (see section 2.2) and more recently published opacity tables.

5.2. The effective temperature

Figure 8 illustrates how $T_*(L_*, M_*, M_\mathrm{c})$ depends on the various variables and physical model assumptions. Let us first discuss the standard case (pop I, $M_* = 1$, MLT; upper left box). For a given core mass, t_* decreases almost linearly for increasing l_* as known from the Hayashi theory, the exact value of the slope depending on the opacity as a function of P and T, here $\mathrm{d}t_*/\mathrm{d}l_* \approx -0.2$. When l_* approaches the Eddington luminosity (L_Edd), t_* becomes locally almost independent of l_*, and there is even a bending towards hotter t_* for large M_c. Such mantles are no longer fully convective. It is obvious that the pressure at the photosphere has a minor influence (dotted lines, upper left

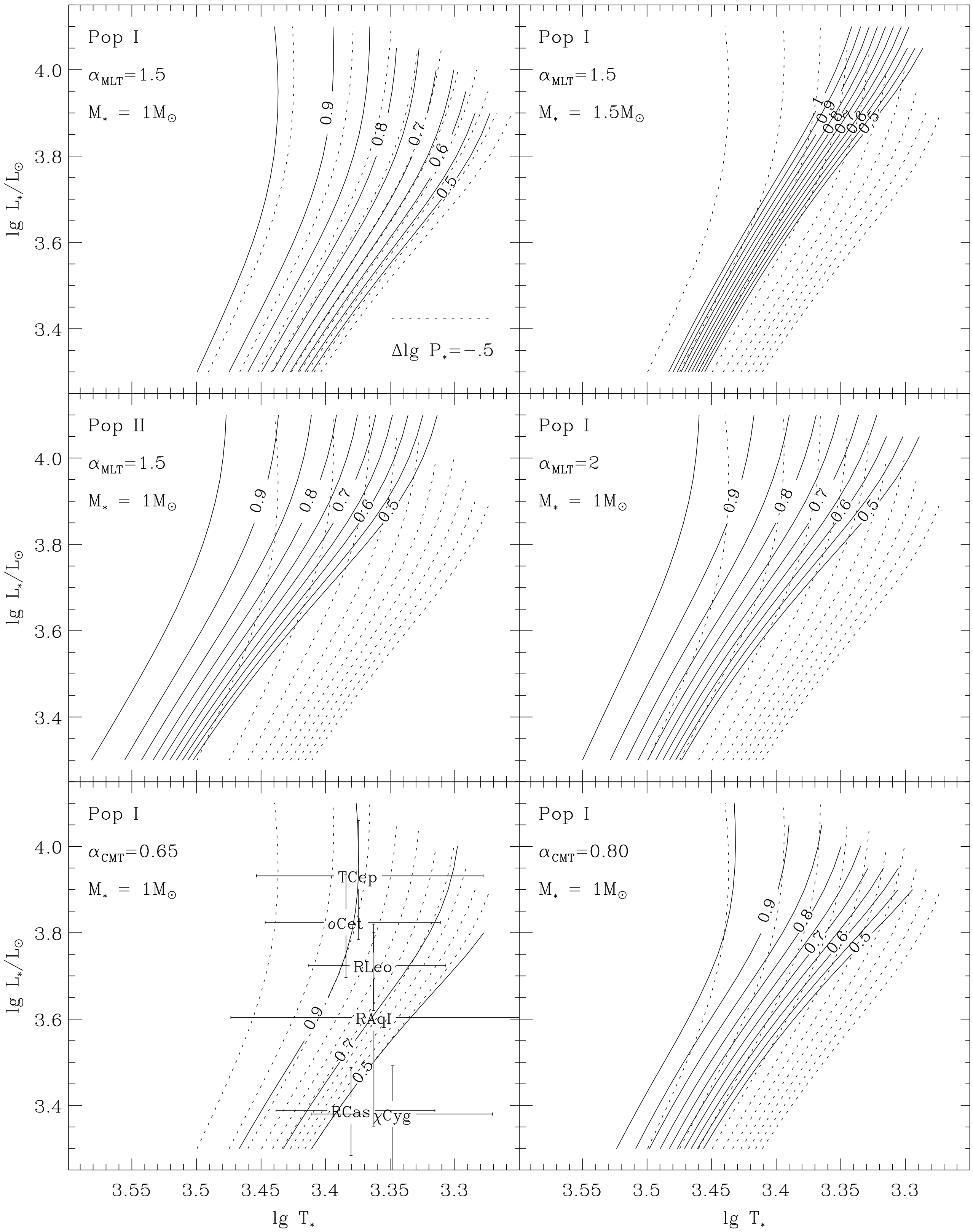

Fig. 8. The effective temperature as a function of L_*, M_*, M_c and Z, and the influence of various model assumptions by means of the example $M_* = 1$. The standard case is depicted in the upper left box; the full lines are $T_*(L_*)$ for $M_c = 0.5, \ldots, 0.95M_\odot$. This case is repeated in all other boxes as dotted lines for comparison. In the upper left box itself, the dotted lines are obtained by reducing the pressure at the outer boundary condition by a factor of three as compared to the usual relation $P_*(L_*, M_*, T_*)$. In the lower left box, recent observational data (see text) are overplotted with 1σ error boxes.

box), since on the AGB for $l_* > 3$, $p_* < 3$ for all atmosphere models considered.

If the mantle mass is reduced, i. e. for growing M_c with M_* kept constant, t_* *increases*. The influence of M_c on t_* is the less pronounced the larger M_* is; for $M_* \gtrsim 2$ it is already almost negligible. Increasing M_*, while M_c = const, leads to higher effective temperatures and vice versa without changing $\mathrm{dt}_*/\mathrm{dl}_*$ significantly (upper right box). This effect is responsible for the trend towards lower effective temperatures on the upper AGB as the objects lose mass, as long as $M_\mathrm{m} \gtrsim 0.2$. If M_m becomes smaller, the former effect takes over, and for $M_\mathrm{c} \approx$ const a shrinking total mass leads to *higher* T_*, and thus to the departure of proto-PN objects from the AGB.

Increasing the MLT parameter has nearly the same effect as reducing the metallicity (middle row): it shifts the whole set of curves towards higher effective temperatures without changing the influence of M_c. It turns out that there is no qualitative difference between the MLT and the Canuto-Mazzitelli theory (1991, CMT, lower row). Quantitatively, there is no single value of α_CMT which reproduces $t_{*,\mathrm{MLT}}$ for all M_c and l_* to within 300K. This difference, however, is much smaller than the errors of the available observational determinations of t_*. Recent data (van Leeuwen et al., 1997) that make use of HIPPARCOS parallaxes, shown in the lower left box of Fig. 8, support the lower T_*-scale. E. g. χ Cyg can well be explained to be a low-mass object ($M_* \approx 0.75$) with a low-mass progenitor, so that $M_{\mathrm{c},0} \approx 0.535$, in one of its first TPCs ($M_\mathrm{c} = 0.540$).

5.3. The bottom of the convective mantle

With respect to HBB, $T_\mathrm{b}(L_*, M_*, M_\mathrm{c})$ together with ρ_b determines the rate of nuclear reactions (see e. g. Scalo, Despain & Ulrich, 1975). A fact that has been widely disregarded in the past is that also the steepness of the T- and P-profiles is decisive for HBB, since it, together with the mixing time scale, determines the amount of matter subject to burning. There are two extreme possibilities: On the one hand, the fuel could be burnt locally at the bottom of the mantle convection zone. On the other hand, if the mixing is sufficiently effective, the mantle material as a whole at any instant of time could be subject to nuclear processing. The local mixing time scales, which are very poorly known from the MLT, determine the actual situation between these extremes. As long as the uncertainties due to the convection formalism dominate to such an extent, it is well justified to use parametrized descriptions instead of time consuming full stellar evolution calculations.

The most important quantity is of course the temperature at the base of the convective mantle (Fig. 9, upper left box). The present work qualitatively confirms the results obtained by Boothroyd, Sackmann & Ahern (1993) by means of full stellar evolution calculations, and work out the basic dependencies more clearly, like the shift of T_b caused by breathing pulses (their Figure 1c), which can be easily explained as the effect of an increased core mass.

For sufficiently large total masses $M_* \gtrsim 2$, t_b is roughly independent of M_*. Cool bases ($t_\mathrm{b} \lesssim 7$) occur for $l_* \lesssim 4$. If the luminosity increases beyond some critical value depending on M_c, T_b either rises approximately like $T_\mathrm{b} \propto L_*^5$ for low core masses, or drops, since the inner parts of the mantle become radiative for large M_c and small M_* (in Fig. 9, this is the case for $l_* > 4.2$, $M_* = 3$ and $M_\mathrm{c} \geq 0.7$). At $t_\mathrm{b} \approx 7.9$, the rise flattens, unless l_* gets very close to the Eddington luminosity. For a given set of opacity tables, "hot bottoms" can occur for sufficiently large luminosities only if the ratio $\frac{M_\mathrm{c}}{M_*}$ is *less* than some constant that depends solely on Z and the convection description. A useful approximation is

$$\frac{M_\mathrm{c}}{M_*} < \begin{cases} 0.2\,\alpha_\mathrm{MLT} - 5Z, & \text{for MLT, and} \\ 0.5\,\alpha_\mathrm{CMT} - 5Z - 0.08, & \text{for CMT.} \end{cases} \tag{21}$$

The influence of the physical models is only moderate (Fig. 9, upper right box) and leads predominantly to a shift of $t_\mathrm{b}(l_*)$ along the l_*-axis, which is equivalent to a rescaling of M_c. Every change of the physical model input that leads to higher effective temperatures, like lower opacities at low temperatures, lowers the threshold for l_* above which HBB takes place. Changes of the opacities $\kappa(T, P)$ can be compensated by varying α appropriately, as can be clearly seen for the pair of cases shown with long dashed and thick dotted lines. For the former, CMT and $\alpha_\mathrm{CMT} = 0.80$ was used, for the latter MLT, $\alpha = 1.5$ and recent OPAL opacities with low temperature extensions according to Alexander & Ferguson (1994, labelled AF94 in the figure). For the pop II models, which imply a drastic reduction of κ at low temperatures, also the plateu value of t_b is increased significantly (dotted lines in Fig. 9, upper right box).

In order to calculate nuclear reaction rates, the density at the convective base must be given, too. Since the mantle convection zones are almost entirely adiabatic, ρ_b also fixes the entropy. For a sufficiently large total mass, and unless L_* approaches the Eddington limit, the simple relation

$$\lg \frac{T_\mathrm{b}^3}{\rho_\mathrm{b} L_*} = 18.9 - 0.4 M_\mathrm{c} \tag{22}$$

holds remarkably well over one order of magnitude of L_* (Fig. 9, upper middle row) and may be used to estimate ρ_b.

As has been already mentioned, the quantity $\left.\frac{\mathrm{d\,lg\,T}}{\mathrm{dM_r}}\right|_\mathrm{b}$ (Fig. 9, lower middle row) determines the amount of matter subject to nuclear processing. It increases approximately as $\propto L_*^3$, and even superexponentially when $L_* \to L_\mathrm{Edd}$. This means, that the effect of reaching very high base temperatures could be entirely compensated by the fact that almost no fuel is left. It must be emphasized, that the nuclear yields will depend extremely sensitively on the mixing time scales in such a situation, which are not correctly predicted by the MLT!

In the lower row of the figure, the adiabatic gradient $\nabla_\mathrm{ad,b} \equiv \left.\frac{\mathrm{d\,ln\,T}}{\mathrm{d\,ln\,P}}\right|_\mathrm{ad,b}$ is shown. Let $h \equiv \left.\frac{\mathrm{d}\ln\rho}{\mathrm{d\,ln\,T}}\right|_\mathrm{b}$, with $1.8 \lesssim h \leq 3$, denote the steepness of the density profile. Then $\nabla_\mathrm{ad,b}$, the ratio β of the gas pressure to the total pressure, including that of radiation, and h are (exactly) connected by the relations

$$\nabla_\mathrm{ad,b} = \frac{3}{4}\frac{2h - 7}{2h^2 - 6h - 3} = \frac{4 - 3\beta}{16 - 12\beta - \frac{3}{2}\beta^2} \tag{23}$$

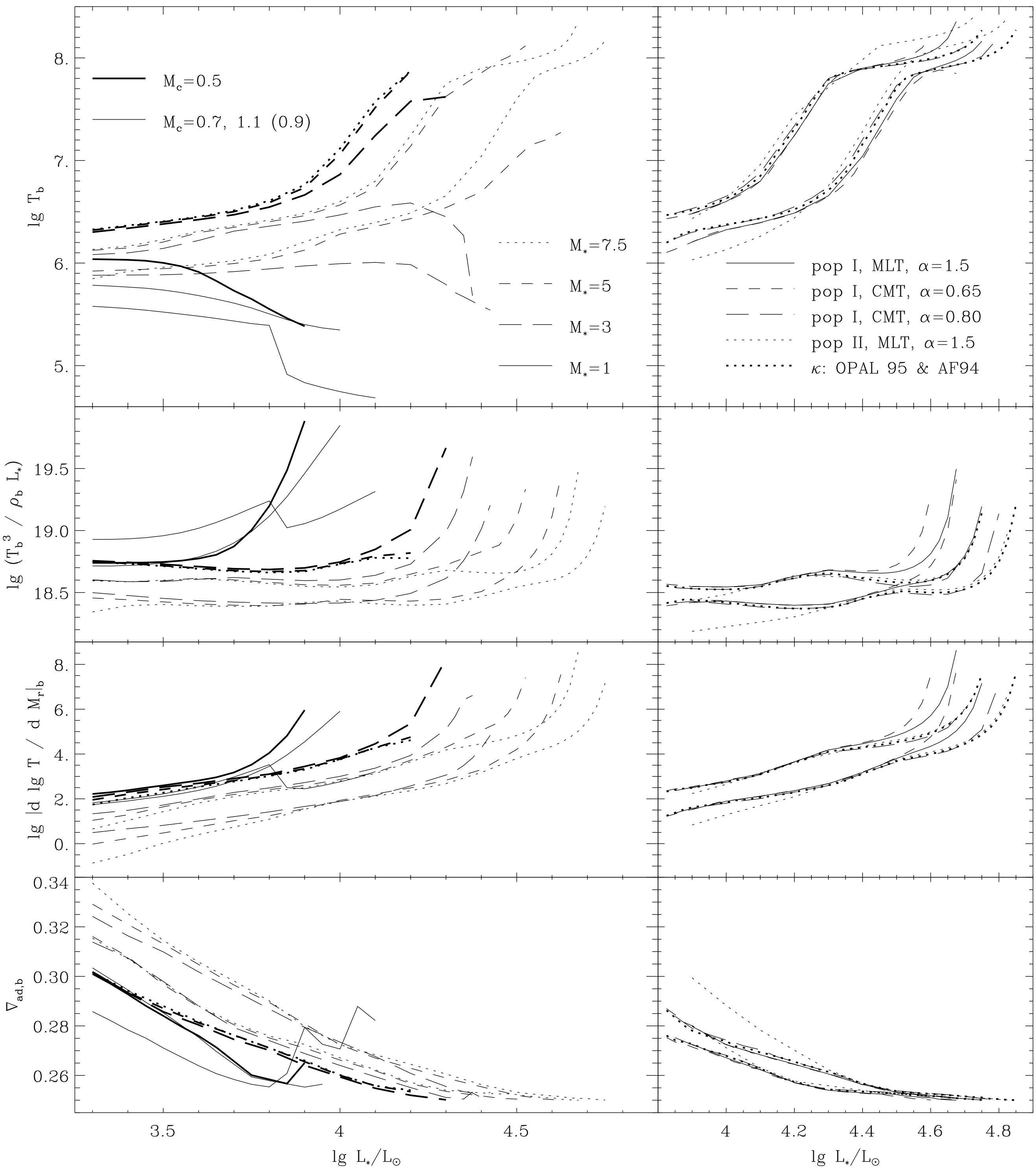

Fig. 9. The temperature and some quantities characterizing the overall conditions at the bottom of the convective mantle (see text) as functions of L_*, M_* and M_c for the standard case (pop I, MLT, α = 1.5, left column) and for various physical assumptions (right column). Left: the thick lines show the data for M_c = 0.5 and different total masses as indicated. The thin lines illustrate the effect of M_c (for M_* = 1, the highest core mass is $0.9M_\odot$, in all other cases $1.1M_\odot$). Right: The same quantities for M_* = 7.5 and M_c = 0.7 and 1.1 (left resp. upper bunch of curves) for various physical model assumptions.

as long as degeneracy plays no role for the EOS. In any case, $\rho_{\rm b} < 10{\rm g~cm}^{-3}$, so that this assumption is well fulfilled. The uniform decrease of $\nabla_{\rm ad,b}$ as L_* increases demonstrates the increasing contribution of the radiation pressure to $P_{\rm b}$. For $L_* \to L_{\rm Edd}$, $\beta \to 0$ and $\nabla_{\rm ad,b} \to 0.25$. $t_{\rm b}(l_*)$ reaches the plateau value of $t_{\rm b} \approx 7.9$ approximately when the radiation pressure dominates, $\beta < 1/3$, or $\nabla_{\rm ad,b} < 0.255$.

6. Summary

We present analytical formulae that describe the evolution of a star on the AGB. This outdates all previous work on this subject up to now for several reasons. First, all formulae are based on a homogeneous set of up-to-date full stellar evolution models that cover all relevant masses and a large range in metallicity. Second, the analytical formulae take into account several important features found in the full calculations, and largely neglected so far in previous analytical descriptions: the secular variations of the luminosity during a thermal pulse cycle, turn-on effects during the first few pulses, and hot bottom burning.

In future work we plan to include a description of the variations of the various chemical species during 1st, 2nd and 3rd dredge-up and HBB, which were not addressed in the full stellar evolution models.

We are currently writing a numerical code to implement the analytical formulae described in this paper. When the chemical description is included we are in a position to improve upon the AGB population synthesis models of GdJ or Marigo et al. (1996). With such a code we are also in a position to investigate new data on AGB stars in extragalactic systems that will become available with the current and new generation of 8-10m telescopes.

Acknowledgements. JW is indebted to Dr. Achim Weiss for comments on the manuscript and his general effort for him at the MPA. MG acknowledges help from Henrik Spoon (MPE) in understanding IDL at a very late stage in the preparation of this manuscript.

References

Alexander D.R., Ferguson J.W., 1994, ApJ 437, 879 (AF94)
Anders E., Grevesse N., 1989, Geochimica et Cosmochimica acta 53, 197
Arnett W.D., 1969, Ap & Sp. Sci. 5, 180
Blöcker T., 1995, A&A 297, 727 (B95)
Boothroyd A.I., Sackmann I.-J., 1988, ApJ 328, 632 (BS88)
Boothroyd A.I., Sackmann I.-J., Ahern S.C., 1993, ApJ 416, 762
Canuto V.M., Mazzitelli I., 1991, ApJ 370, 295 (CMT)
Cassisi S., Castellani V., Tornambè A., 1996, ApJ 459, 298
Castellani V., Chieffi A., Pulone L., Tornambè A., 1985, ApJ 296, 204
Castellani V., Chieffi A., Straniero O., 1990, ApJS 74, 463 (CC90)
D'Antona F.D., Mazzitelli I., 1996, ApJ 470, 1093 (DAM96)
Fleischer A.J., Gauger A., Sedlmayr E., 1992, A&A 266, 321
Frost C., Lattanzio J., 1996, ApJ 473, 383
Groenewegen M.A.T., de Jong T., 1993, A&A 267, 410 (GdJ)
Groenewegen M.A.T., de Jong T., 1994, A&A 283, 463
Groenewegen M.A.T., van den Hoek L.B., de Jong T., 1995, A&A 293, 381
Herwig F., Blöcker T., Schönberner D., El Eid E., 1997, A&A 324, L81
Iben I. Jr, Renzini A., 1983, Ann. Rev. A&A 21, 271
Iben I. Jr, Truran J.W., 1978, ApJ 220, 980 (IT78)
Jimenez R., MacDonald J., 1998, MNRAS, submitted
Jørgensen U.G., 1991, A&A 246, 118
Kippenhahn R., Weigert A., 1990, Stellar Structure and Evolution, Springer, Berlin
Lattanzio J.C., 1986, ApJ 311, 708 (LA86)
Marigo P., Bressan A., Chiosi C., 1996, A&A 313, 545
Mazzitelli I., D'Antona F., 1986, ApJ 308, 706
Mowlavi N., Jorissen A., Arnould M., 1996, A&A 311, 803
Olofsson H., Carlström U., Eriksson K. et al., 1990, A&A 230, L13
Paczyński B., 1970, Acta Astr. 20, 47
Paczyński B., 1975, ApJ 202, 558
Pagel B.E.J., 1992, in: Sanchez F., Collados M., Rebolo R. (eds.), Observational and physical cosmology, Cambridge Univ. Press
Reimers D., 1975, Mem. Soc. Roy. Liège, 6, VIII, 369
Renzini A., Voli M., 1981, A&A 94, 175
Rogers F.J., Iglesias C.A., 1992, ApJS 79, 507
Russell S.C., Bessell M.S., 1989, ApJS 70, 865
Russell S.C., Dopita M.A., 1990, ApJS 74, 93
Scalo J.M., Despain K.H., Ulrich R.K., 1975, ApJ 196, 805
Schönberner D., 1979, A&A 79, 108
taniero O., Chieffi A., Limongl M., et al., 1997, ApJ 478, 332
Tuchman Y., Sack N., Barkat Z., 1979, ApJ 234, 217
van Leeuwen F., Feast M.W., Whitelock P.A., Yudin B., 1997, MNRAS 287, 955
Vassiliadis E., Wood P.R., 1993, ApJ 413, 641 (VW93)
Vassiliadis E., Wood P.R., 1994, ApJS 92, 125
Wagenhuber J., 1996, PhD thesis, TU München
Wagenhuber J., Tuchman Y., 1996, A&A 311, 509
Wagenhuber J., Weiss A., 1994, A&A 286, 121 (WW94)
Weiss A., Keady J.J., Magee N.H., 1990, Atomic Data and Nuclear Data Tables 45, 209
Weiss A., Truran J.W., 1990, A&A 238, 178
Weiss A., Wagenhuber J., Denissenkov P.A., 1996, A&A 313, 581
Wood P.R., Faulkner, D.J., 1986, ApJ 307, 659
Wood P.R., Zarro D.M., 1981, ApJ 247, 247 (WZ81)

This article was processed by the author using Springer-Verlag LaTeX A&A style file *L-AA* version 3.